Kinetic Analysis of the Role of Zinc in the Interaction of Domain 5 of High-Molecular Weight Kininogen (HK) with Heparin†

Yingzhang Lin,‡ Robin A. Pixley,‡ and Robert W. Colman*

Sol Sherry Thrombosis Research Center, Temple University School of Medicine, Philadelphia, Pennsylvania 19140

Received August 31, 1999; Revised Manuscript Received February 23, 2000

ABSTRACT: Previous investigations have shown that HK and its light chain bind heparin, preventing the enhancement of antithrombin inhibition of thrombin and potentiating the inhibition of plasma kallikrein by antithrombin. We found that both HK and HKa bound heparin, but HK exhibited a greater affinity. We therefore localized the binding sites for heparin on HK. HK domains 5 and 6 of the light chain as well as domain 3 from the heavy chain, expressed as glutathione *S*-transferase (GST) fusion proteins in *Escherichia coli*, were tested for binding to immobilized heparin by surface plasmon resonance using a BiaCore 2000 instrument. GST-D5, but not GST-D3, GST-D6, or GST, bound to heparin when the recombinant domains were present at a concentration of 70 nM. To localize more precisely the amino acid sequences on D5, both of the subdomains, histidine-glycine-rich GST-(K420−D474) and histidine-glycine-lysine-rich GST-(H475−S626), were expressed and tested for binding to immobilized heparin. The K_d was much lower for GST-(K420−D474) than for GST-(H475−S626) in the presence or absence of Zn^{2+}. GST-(K420−D474) was effective in decreasing the rate of inactivation of thrombin by antithrombin in the presence of heparin and Zn^{2+}, while GST-(H475−S626) had no effect. We conclude that the binding of heparin to HK is a complex function of Zn^{2+} interacting with histidines in the sequence K420−D474 to create high-affinity binding sites. HK has the potential to be an important modulator of heparin therapy.

HK is a multidomain molecule with many functions, each mediated by binding to different ligands. HK is cleaved by plasma kallikrein to form cleaved HK (HKa) (*1*), a disulfide-bonded two-chain molecule, bradykinin (amino acids 363−371), and a polypeptide (amino acids 372−419). The N-terminal heavy chain common to HK and low-molecular weight kininogen (LK) contains three domains homologous to crystalline cystatin. Domain 1 binds Ca^{2+}; domain 2 binds to and inhibits platelet calpain (*2*, *3*), and domain 3 (D3) binds to receptors on platelets (*4*), neutrophils (*5*), and endothelial cells (*6*), thereby inhibiting thrombin binding to platelets (*7*, *8*), accounting for HK antithrombotic action in vivo (*9*). Domain 5 (D5) contains two subdomains, a histidine-glycine-rich region (amino acids 420−474) and a histidine-glycine-lysine-rich region (amino acids 475−502) (Figure 1) which bind to cellular receptors (*5*, *6*, *10*, *11*) as well as to anionic surfaces (*12*). D5 is also responsible for the antiadhesive action of HKa on neutrophils (*13*, *14*) and endothelial cells (*15*). Finally, domain 6 (D6) binds prekallikrein and kallikrein (*16*) and is required for prourokinase-activated fibrinolysis on endothelial cell surfaces (*17*).

Heparin has been shown to bind to HK and HKa, but not to LK (*18*), implying that the binding site is in the light chain of HKa. Heparin binding was quantified by the ability of

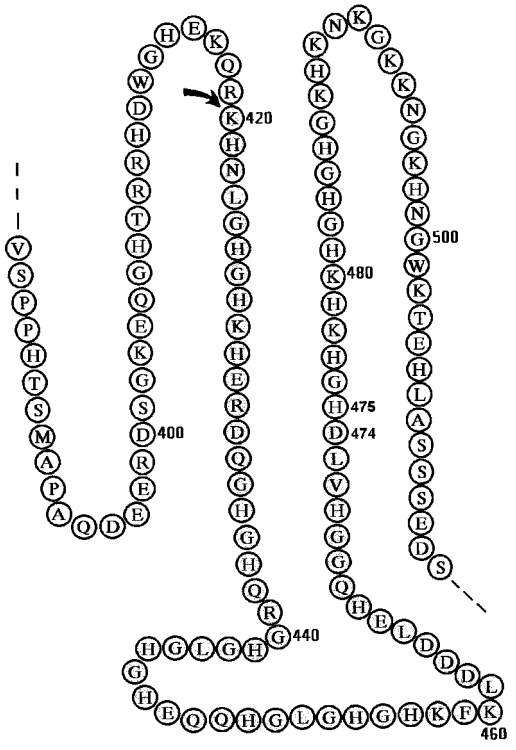

FIGURE 1: Structure of D5 of HK. D5 is the high-molecular weight kininogen domain composed of V383−K502. The arrow indicates the location of the third kallikrein cleavage site in the HK molecule. GST-D5 used in this study is the GST N-terminally linked to K420−S513. Two D5 sequences, expressed as recombinant GST fusion proteins in this study, are K420−D474 and H475−K502.

HK to inhibit the heparin-induced enhancement of antithrombin inhibition of thrombin. Zn^{2+} at a concentration of

† The work was supported by grants from NIH, P01 HL56914 and CA 83121 (R.W.C.), and the American Cancer Society, ACS-IRG-204 (Y.L.).

* To whom correspondence should be addressed: Sol Sherry Thrombosis Research Center, Temple University School of Medicine, 3400 N. Broad St., Philadelphia, PA 19140. Telephone: (215) 707-4665. Fax: (215) 707-2783. E-mail: colmanr@astro.temple.edu.

‡ These authors contributed equally to this work.

10.1021/bi992048z CCC: $19.00
Published on Web 04/05/2000

10 μM inhibited the heparin enhancement of thrombin inhibition by HK (200 nM) to the level of the uncatalyzed reaction, indicating indirectly that Zn^{2+} enhances heparin binding to HK. However, the regions of the light chain of HKa which support heparin binding have not been elucidated, nor has the action of zinc been clearly defined. This action of heparin has further functional implications, since Olson et al. (*19*, *20*) have shown that HK enhances the ability of antithrombin to inhibit kallikrein and enhances prekallikrein activation.

Therefore, using surface plasmon resonance, we studied the binding of HK, HKa, recombinant domains 3, 5, and 6, and recombinant subdomains of D5 (see above) to define the sequences that are responsible in HK for binding heparin, as well as the role of Zn^{2+} in the association and dissociation reactions.

MATERIALS AND METHODS

HK and HKa were purchased from Enzyme Research Laboratories (South Bend, IN). HK was >95% of a single band of 110 kDa on both nonreduced and reduced SDS electrophoresis. HK had been digested with plasma kallikrein (molar ratio of 100:1 of HK to plasma kallikrein) for 20 min at 37 °C. The resulting HKa was composed of two bands of 62 and 46 kDa, when analyzed by reduced SDS electrophoresis. The band of 62 kDa (amino acids 1−362) represents the heavy chain of HK, while the 46 kDa band represents the smaller light chain following the third cleavage by plasma kallikrein (amino acids 420−626). Antithrombin was purchased from Enzyme Research Laboratories. Human α-thrombin was a generous gift from John W. Fenton, II (Division of Laboratories and Research, New York State Department of Health, Albany, NY) and had a specific activity of 2400 NI4 units/mg and a purity of 99.24%. S-2238 (H-D-phenylalanyl-L-pipecoyl-L-arginyl-*p*-nitroaniline hydrochloride) was purchased from DiaPharma Group, Inc. (West Chester, OH).

Recombinant Proteins. Deletion mutants of the light and heavy chains of HK were prepared as previously described (*21*). These have been constructed in pGEX2T vectors using a cDNA, encoding the light and heavy chains of human HK as targets for restriction enzymes. Each construct has glutathione *S*-transferase (GST) at the N-terminus of the polypeptide fused to the HK polypeptide. The amino acid sequences linked to GST for GST-D3, GST-D5, and GST-D6 are K236−M357, K420−S513, and S565−S626, respectively. We also constructed two deletion mutants of D5, both linked to GST, K420−D474, which lacks the histidine-glycine-lysine-rich region, and H475−S626, which lacks the histidine-glycine-rich region. The mutants were purified on a glutathione column to >90% purity as previously described (*21*).

Biotinylation of Heparin. Homogeneous low-molecular weight heparin (10 mg) (molecular weight of 9000), purchased from Enzyme Research Laboratories, was dissolved in 2.5 mL of 0.1 M sodium acetate and 0.15 M NaCl (pH 5.5) and chilled on ice, and 50 mL of 0.5 M sodium periodate was added. After mixing, it was returned to an ice bath and placed in the dark for 20−30 min. Fifty milliliters of 1 M sodium sulfite solution was added to stop the oxidation. The oxidized heparin was applied to a PD-10 column which had been pre-equilibrated in the acetate buffer and concentrated to a volume of 0.9 mL using a Centricon-3 apparatus. One hundred milliliters of an 8 mg/mL biotin-x-x-hydrazide solution (in dimethylformamide) was added to 0.9 mL of concentrated oxidized heparin, mixed, and incubated at 25 °C for 24 h. The excess biotin was removed using a Centricon-3 apparatus.

Surface Plasmon Resonance Analysis. Real-time biomolecular interaction analysis was performed by using a BiaCore 2000 instrument (*22*). Binding data were collected with a thermostated resonant mirror biosensor. All of the experiments were performed at 25 °C using the buffer containing 20 mM HEPES and 0.15 M NaCl (pH 7.4). The flow rate was 10 μL/min unless otherwise specified.

Immobilization of Biotinylated Heparin for BiaCore Analysis. Biotinylated heparin (∼9 kDa) was immobilized upon a gold−dextran surface to which streptavidin from *Streptomyces adidinii* had been covalently bound (SA-5 sensor chip). Heparin (1 μg/mL) in 20 mM HEPES and 0.15 M NaCl (pH 7.4) was then injected at a flow rate of 5 μL/min. Nonspecifically bound heparin was removed by a wash with 1 M NaCl. Approximately 50−150 resonance units (RU) (∼50−150 pg/mm^2) of heparin was bound to the chip for the study of HK, HKa, GST-D5, GST-D3, GST-D6, GST-(K420−D474), and GST-(H495−S626).

Kinetic Analysis of Heparin Interaction with HK, HKa, GST-D5, GST-(K420−D474), and GST-(H495−S626). HK, HKa, GST-D5, GST-(K420−D474), and GST-(H495−S626) were perfused across an SA-5 chip upon which biotin−heparin had previously been immobilized as described above at a flow rate of 10 mL/min for 50−350 s. At least five different concentrations of each protein were injected. After each analyte injection, the chip surface was regenerated by perfusion with 4 M $MgCl_2$ for 2 min and then with 1 M NaCl for 3 min. This regeneration protocol reproducibly brought RU values back to those observed before analyte perfusion.

Binding of proteins to the streptavidin−gold−dextran surface is expressed in resonance units (1 RU ∼ 1 pg/mm^2). Changes in RU over time form a "sensorgram", and these changes have been shown to be proportional to the changes in mass bound to the surface. Data were analyzed by BIAevaluation 3.0 software. A Langmuir binding model (stoichiometry of 1:1) was used to analyze k_{on} (association rate constant, M^{-1} s^{-1}), k_{off} (dissociation rate constant, s^{-1}), and K_D (equilibrium dissociation constant) for HK, HKa, GST-D5, and GST-D5 subdomains binding to heparin. For each concentration, k_{on} and k_{off} were obtained simultaneously from the equation $K_D = k_{off}/k_{on}$.

Thrombin−Antithrombin Assay. Combinations of antithrombin, expressed GST-HK peptide, and heparin were incubated at room temperature in a 1.5 mL polypropylene centrifuge tube in a buffer of 0.01 M HEPES, 0.1 M NaCl, and 0.1% PEG 8000 (pH 7.4) containing 10 μM $ZnCl_2$ or 100 μM EDTA. After thrombin was added to give a final volume of 300 μL, 30 μL aliquots were removed at specified times and placed in a Falcon 96 microtiter plate well containing the thrombin substrate, S-2238, to measure remaining thrombin catalytic activity. Each well contained 300 μM S-2238 in a volume of 100 μL in a buffer of 0.02 M HEPES, 0.25 M NaCl, 100 μM EDTA, 0.1% PEG 8000, and 100 μg/mL hexadimethrine bromide (pH 7.4). The

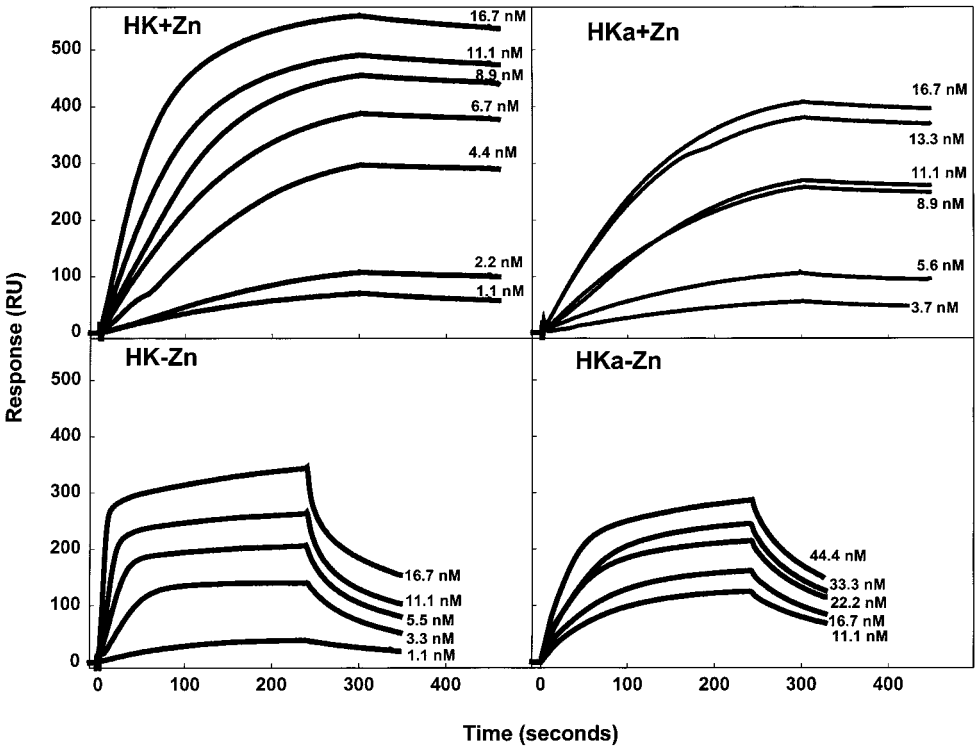

FIGURE 2: Surface plasmon resonance sensorgram of the association and dissociation of HK and HKa with immobilized heparin. Biotinylated heparin (50 RU) was immobilized on an SA-5 streptavidin-coated dextran chip and perfused with buffer [20 mM HEPES and 0.15 M NaCl (pH 7.4)] at a rate of 10 μL/min. The binding affinities of HK (at 1.1−16.7 nM) and HKa (at 11.1−44.4 nM) were determined with (top) and without (bottom) $ZnCl_2$ (50 μM). The k_{on} and k_{off} were calculated on the basis of the rate of change of RU vs time and are shown in Table 1.

Table 1: Kinetic Constants of HK, HKa, GST-D5, GST, GST-(K420−D474), and GST-(H475−S626)[a]

	with Zn^{2+} (50 μM $ZnCl_2$)			without Zn^{2+} (with 50 μM EDTA)		
	K_D (nM)	k_{on} (M^{-1} s^{-1}) ($\times 10^6$)	k_{off} (s^{-1}) ($\times 10^{-4}$)	K_D (nM)	k_{on} (M^{-1} s^{-1}) ($\times 10^6$)	k_{off} (s^{-1}) ($\times 10^{-4}$)
HK	0.30 ± 0.07	1.27 ± 0.81	4.03 ± 3.53	2.11 ± 0.71	3.38 ± 0.55	69.0 ± 17.0
HKa	1.39 ± 1.20	0.53 ± 0.19	6.87 ± 5.43	14.2 ± 5.28	0.54 ± 0.17	69.8 ± 3.78
GST-D5-(K420−S513)	5.14 ± 1.69	0.06 ± 0.01	2.92 ± 1.30	27.7 ± 22.3	0.02 ± 0.02	4.42 ± 1.64
GST-(K420−D474)	3.53 ± 0.68	0.012 ± 0.005	0.314 ± 0.098	1.56 ± 0.40	0.04 ± 0.01	0.80 ± 0.12
GST-(H475−S626)	11.9 ± 1.7	0.030 ± 0.004	0.339 ± 0.039	52.6 ± 4.9	0.010 ± 0.001	5.37 ± 0.52
GST	>1300	NA	NA	>1300	NA	NA

[a] Mean ± SD, χ^2 range of 0.35−45.0, NA, not analyzable. Independent fits using Langmuir 1:1 kinetics. Buffer: 0.01 M HEPES and 0.15 M NaCl at pH 7.4 and 25 °C.

reaction with thrombin was allowed to proceed at room temperature for exactly 15 min, at which time 100 μL of 50% acetic acid was added to stop the reaction. The plate was read at 405 nm on an EL808U Ultra Microplate Reader (Bio-Tek Instruments, Inc., Winooski, VT) to assess the generation of pNA from the substrate. A standard curve using different concentrations of thrombin alone was generated to convert the unknown to thrombin concentrations.

RESULTS

Effect of Zn^{2+} on HK or HKa Binding to Immobilized Heparin. We first studied the binding of HK and HKa. The binding affinity was determined at different protein concentrations with and without the addition of $ZnCl_2$ (50 μM). In the absence of Zn^{2+}, HK displays a higher affinity (K_D = 2.1 nM) for immobilized heparin than HKa with a K_D of 14.2 nM (Figure 2 and Table 1). HK and HKa both increase the affinity of binding to heparin by about 10-fold in the presence of Zn^{2+}: K_D = 0.30 nM for HK and K_D = 1.39 nM for HKa (Figure 2 and Table 1). The increase in binding affinity is attributed to the lower K_{off} for both molecules in the presence of Zn^{2+}, while Zn^{2+} has little effect on k_{on} for either HK or HKa (Figure 3 and Table 1).

Comparison of the Binding Affinity for D3, D5, and D6. To determine which domain bound to heparin, we then compared GST fusion proteins of the two cell binding domains of HKa, D3 and D5, and the kallikrein binding domain, D6. Domain 5 is in the histidine-lysine-glycine-rich region of HK. At either high or low concentrations, GST-D5 shows the highest affinity of binding to immobilized heparin, while GST-D3, GST-D6, and GST alone bound very poorly, and to about the same extent (Figure 4). We then performed a kinetic analysis of the binding of GST-D5 to immobilized heparin in the presence of Zn^{2+} at concentrations from 4.4 to 20.4 nM (Figure 5). For GST-D5 with Zn^{2+}, $k_{on} = 0.06 \times 10^6$ M^{-1} s^{-1}, $k_{off} = 2.92 \times 10^{-4}$ s^{-1}, and K_D = 5.14 nM. In the absence of Zn^{2+}, the extent of binding was reduced and concentrations of GST-D5 of 18−135 nM were

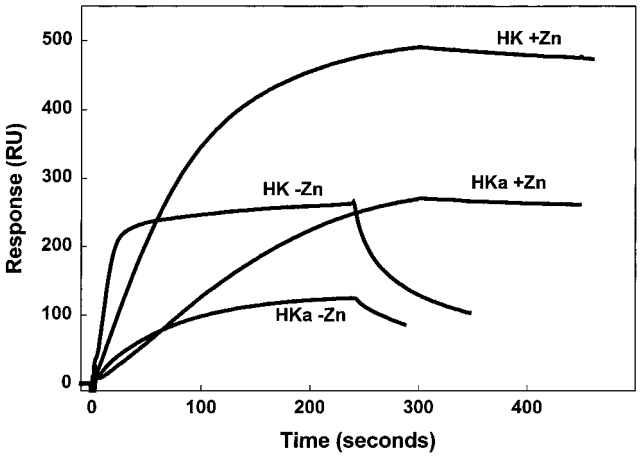

FIGURE 3: Representative sensorgrams of HK and HKa binding to heparin in the presence and absence of zinc. The binding of HK and HKa to heparin was assessed in the presence of 50 μM $ZnCl_2$ and its absence at a concentration of 11.1 nM. The k_{on} of HK was greater than that of HKa. The k_{off} in the presence of zinc was 10-fold greater than in its absence with both HKa and HK.

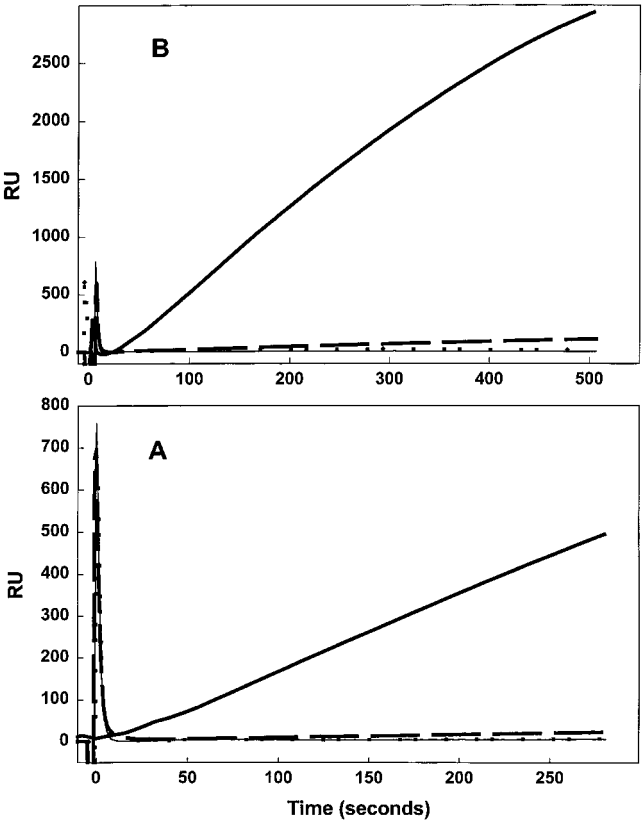

FIGURE 4: Binding affinity of GST, GST-D3, GST-D5, and GST-D6 to immobilized heparin in the presence of 50 μM $ZnCl_2$. Panel A depicts the data generated at lower concentrations. Data for higher concentrations of the same analytes are shown in panel B. Solid lines are GST-D5 at 34 or 200 nM. Dashed lines are GST-D3 at 53 or 297 nM. Dotted lines are GST-D6 at 50 or 335 nM. Thin solid lines are GST alone at 96 or 1300 nM.

used in the binding studies. In the absence of Zn^{2+} for GST-D5, $k_{on} = 0.02 \times 10^6$ M^{-1} s^{-1}, $k_{off} = 0.02 \times 10^{-4}$ s^{-1}, and $K_D = 27.7$ nM (Table 1).

Selection of Recombinants for the Fine Mapping of D5. Because of the involvement of D5 of HK in heparin binding, we attempted to fine map the binding of GST-D5 to heparin using recombinant proteins. We searched the known data-

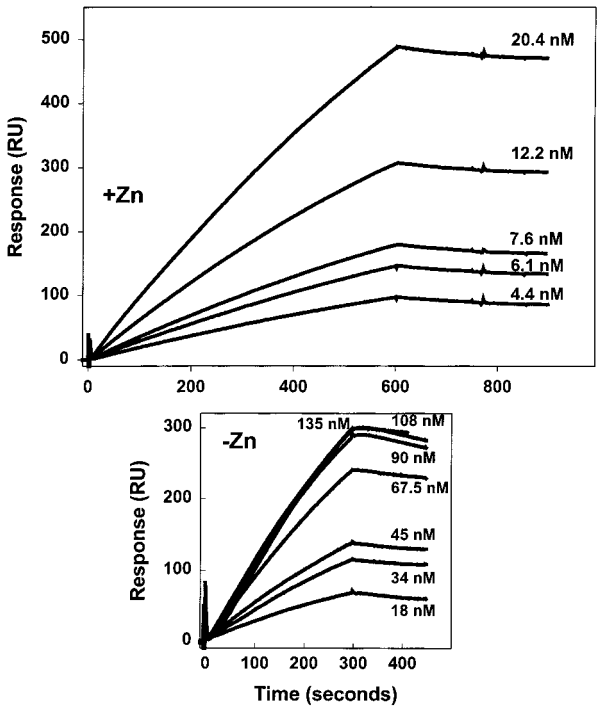

FIGURE 5: Surface plasmon resonance sensorgram of the association and dissociation of GST-D5 with immobilized heparin. In the presence of 50 μM $ZnCl_2$, the concentrations of GST-D5 ranged from 4.4 to 20.4 nM, while in the absence of added Zn^{2+}, higher concentrations of GST-D5 (18−135 nM) were found. k_{on}, k_{off}, and K_D were determined with BIAevaluation 3.0 software using the 1:1 Langmuir binding model.

bases for a suitable template on which to base a homology-modeled structure. D5 of HK is 30.6% identical and 40.5% homologous (identity + similarity) with a histidine-rich actin binding protein, hisactophilin 1, from *Dicytostellium discoideum*. The NMR solution structure for hisactophilin 1 was determined several years ago (*23*, *24*). The structure of the homology model of HK D5 has been published (*25*). The ribbon representation of HK D5 indicates that the core is composed of β-sheets ending in β-turns which represent surface-exposed loops.

Comparison of the Binding Affinity for D5 Deletion Mutants Lacking Subdomains. In a previous study, we defined two subdomains within D5, one rich in histidine and glycine (amino acids 420−475) and the other rich in histidine, glycine, and lysine (amino acids 475−502) (*21*). Each was expressed as a GST fusion protein. The HG-rich region was GST-(K420−D474). Since GST-D6 showed no binding to heparin, GST-(H475−S626), which encompassed the H-G-K-rich region plus D6, was used (Figure 1). Kinetic studies similar to those performed on GST-D3, GST-D5, and GST-D6 were performed using surface plasmon resonance. In the presence of Zn^{2+}, GST-(K420−D474) bound with a higher affinity ($K_d = 3.53$ nM, with $k_{on} = 0.012 \times 10^6$ M^{-1} s^{-1} and $k_{off} = 0.314 \times 10^{-4}$ s^{-1}) than GST-(H475−S626) [$K_d = 11.9$ nM (Table 1)]. The difference was due to a lower k_{on} (0.012×10^6 M^{-1} s^{-1}) since the k_{off} (0.339×10^{-4} s^{-1}) was similar (Figures 6 and 7). In the absence of added Zn^{2+}, the differences were more dramatic, with GST-(K420−D474) binding with a much lower K_d (1.56 nM), a higher k_{on} (0.04×10^6 M^{-1} s^{-1}), and a lower k_{off} (0.80×10^{-4} s^{-1}), than GST-(H475−S626), with a lower affinity ($K_d = 52.6$ nM), a lower k_{on} (0.01×10^6 M^{-1} s^{-1}), and higher k_{off} ($5.37 \times$

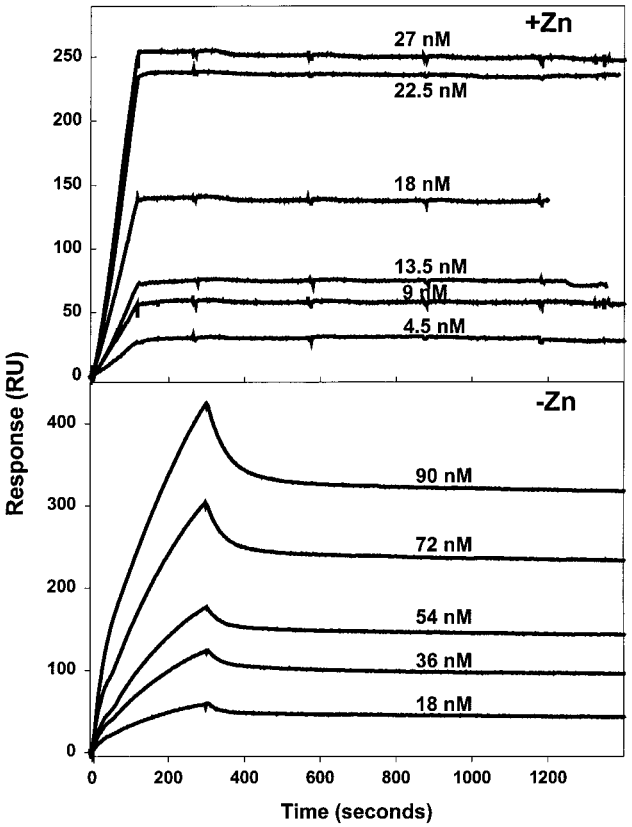

FIGURE 6: Binding of GST-(K420−D474) with immobilized heparin in the presence of zinc. The K_D, k_{on}, and k_{off} were determined with BIAevaluation 3.0 software using the 1:1 Langmuir binding model.

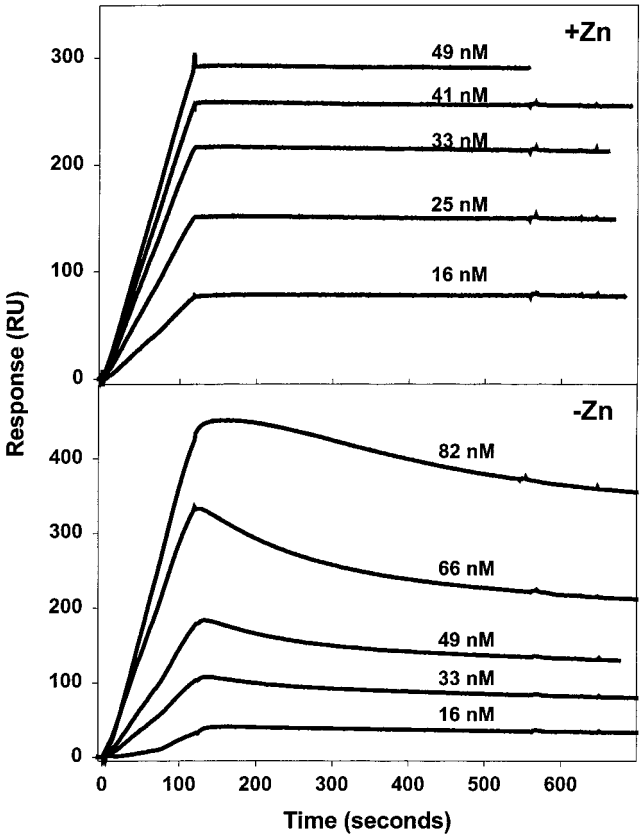

FIGURE 7: Binding of GST-(H475−S626) with immobilized heparin with and without zinc. The K_D, k_{on}, and k_{off} were determined by using the 1:1 Langmuir binding model.

10^{-4} s^{-1}). Thus, GST-(K420−D474) contributes the high-affinity binding of D5. In the presence of EDTA, no binding of GST-(K420−D474) was demonstrated (data not shown). In the buffer used without added zinc, there was detectable Zn^{2+} (<1 μM) (*12*).

Effect of D5 and Its Deletion Mutants on the Heparin-Accelerated Inactivation of Thrombin by Antithrombin. Bjork et al. (*18*) demonstrated that HK, HKa, and its light chain were able to inhibit the rate enhancement by heparin of antithrombin inactivation of thrombin. We confirmed that HK and HKa slowed the heparin-accelerated rate of thrombin inactivation by antithrombin (data not shown). We tested the ability of GST-D5, GST-(K420−D474), and GST-(H475−S626) to decrease the rate of inactivation of antithrombin (236 nM) and of thrombin (12 nM) in the presence of heparin (M_r = 9000, 25 nM) and $ZnCl_2$ (10 μM). In the absence of HK derivatives, we observed the marked acceleration of inactivation of thrombin by antithrombin in the presence of heparin (Figure 8). The rate of inactivation of thrombin by antithrombin with or without heparin was not affected by $ZnCl_2$ (data not shown).

In the presence of D5 and GST-(K420−D474), we found a marked decrease in the rate of inactivation, suggesting that these HK fragments were able to compete with antithrombin or thrombin for heparin binding (Figure 8). The decrease in the rate of concentration did not occur when EDTA was present, suggesting that Zn^{2+} was required for the effect of the HK derivatives. In contrast, GST-(H475−S626) did not affect the rate of inactivation by antithrombin−heparin with or without Zn^{2+} (Figure 8).

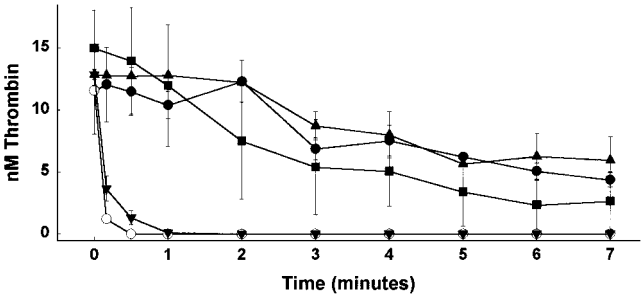

FIGURE 8: Effect of D5 and its deletion mutants on the heparin-accelerated inactivation of thrombin by antithrombin. Antithrombin (AT) at a concentration of 236 nM was incubated in the presence and absence of 100 nM D5 or a deletion mutant and/or 25 nM heparin (Hep) in a 10 μM zinc-containing buffer at room temperature. Thrombin (T) was added to achieve a final concentration of 12 nM in 300 μL. At various time points, an aliquot of the reaction mixture was added to a buffer containing the thrombin substrate, S-2238, to measure residual thrombin activity (see Materials and Methods for details): TAT (●), TATHep (○), TATHep and GST-D5 (■), TATHep and GST-(K420−D474) (▲), and TATHep and GST-(H475−S626) (▼). Mean ± SD (n = 3).

DISCUSSION

Our studies in which we used surface plasmon resonance, a technique with several advantages, have resulted in several new insights into the interactions between HK, heparin, and Zn^{2+}. This technique assesses directly the formation of the complex between heparin and HK or its constituents by an increase in mass. Second, it allows quantitation by calculation of K_D. Surface plasmon resonance is assessed in a flow system, which results in its ability to measure in real time the k_{on} and k_{off}, which may give insight into the nature of

the complex that is formed. Finally, it is appropriate to use immobilized heparin in a flow system, since it closely mimics the interaction of plasma components such as HK with endothelial cell-bound glycosaminoglycans.

Our studies of HK and HKa binding to heparin showed that both species bound surprisingly well. In fact, the binding constants of HK and HKa (K_D = 0.3 and 1.4 nM) compare favorably (K_D = 4.4 nM) to that of platelet factor 4, a protein with a very high affinity for heparin (*26*). HK exhibited a higher affinity (lower K_D) than HKa. This unexpected finding is explained by the loss of amino acids S372−R419 in the formation of HKa by the third cleavage by plasma kallikrein at the R419−K420 linkage. Bjork et al. (*18*) found no difference between HK and HKa, but used an indirect assessment of binding which could have missed this degree of affinity change.

We examined three of the domains of kininogen that react with ligands: GST-D3, which binds to blood cells and endothelial cells; GST-D5, the site for binding to endothelial cells; and GST-D6, the prekallikrein binding site. Only GST-D5 bound to heparin, while GST-D3, GST-D6, and GST did not. This finding directed our attention to GST-D5 as the only domain involved in heparin binding. The enhancement by Zn^{2+} is clear for GST-D5 binding. GST shows no detectable binding. The affinity of D5 is only 5-fold lower than that of HKa, and this domain exhibits most, if not all, of the heparin binding activity, and is potentiated by Zn^{2+}. Retzios et al. (*27*) showed that chemical modification of 14−16 of the 23 available histidines resulted in a decreased level of Zn^{2+} binding as well as binding to anionic surfaces. We have shown that Zn^{2+} increases 5-fold the affinity of a peptide from D5, H441−H458, for anionic surfaces (*12*).

Heparin is a negatively charged polymer (*28*) which interacts with protein molecules via electrostatic interaction with lysines and/or arginines. There are, however, several examples in which zinc, by binding to exposed histidines in protein, facilitates binding to heparin. Zinc acts as a cofactor for heparin neutralization by histidine-rich glycoprotein (*29*). The activation of the plasma kallikrein−kinin system on endothelial cells needs both high-molecular weight kininogen and Zn^{2+} (*30*). In plasma, the total Zn^{2+} concentration is 10−25 μM (*31*). The actual free Zn^{2+} concentration is significantly lower (1−3 μM), since the majority of the ion is bound to albumin (*32*). Because we could determine the individual rate constants of association (k_{on}) and dissociation (k_{off}), we gained insight into the mechanism by which Zn^{2+} tightened the affinity (decreased the K_D for heparin). The k_{on} was minimally increased, but the k_{off} was dramatically decreased for both HK and HKa binding to heparin. This unique observation indicates that Zn^{2+} stabilized the noncovalent complex with heparin.

To begin to map the regions responsible within D5, we took advantage of the fact that while the entire region of amino acids 420−502 was rich in both histidine and glycine, the region of amino acids 475−502 was much richer in lysine. Thus, the region of amino acids 420−474 contains 14 of 55 (26%) histidines, and the region of amino acids 475−502 contains 8 of 28 (28%) histidines, essentially the same. In contrast, the region of amino aacids 420−474 contains 4 of 55 (7%) lysines, while the region of amino acids 475−502 contains 9 of 28 (32%) lysines. Thus, we prepared GST fusion recombinant polypeptides for both of these subdomains and expressed them in *E. coli*. Prokaryotic expression does not allow the evaluation of glycosylation, but there are no consensus sites for attachment of carbohydrate in the sequence of amino acids 420−502, although there are seven probable sites for O-linked carbohydrate in the rest of the light chain and three sites for N-linked carbohydrate in the heavy chain of HK (*33*). We found that in both the presence and absence of added Zn^{2+}, GST-(K420−D474) (Figure 6) contains the sites of high-affinity binding to heparin (K_d = 3.53 and 1.56 nM, respectively) (Table 1). This result is strikingly different from GST-(H475−K502) (Figure 7), which has K_d values of 11.9 and 52.6 nM in the presence and absence of added Zn^{2+}, respectively. In the absence of added Zn^{2+}, the k_{off} for GST-(H475−S626) was 16-fold higher than in the presence of Zn^{2+}, whereas with GST-(K420−D474), the k_{off} was only 2-fold higher. Thus, Zn^{2+} stabilizes the binding of the lysine region, similar to the results without GST-D5. On a surface representation of the homology model (*25*), all histidines appear to be available on the surface and form a localized subdomain. In this case, the cation interacting with the anionic surfaces of heparin serves as a bridge to the zinc-coordinating histidines of D5. Although this mode of heparin binding is rare, it is not unprecedented. Histidine-rich glycoprotein, a close relative of HK, contains homologous regions in both the heavy chain (cysteine protease inhibitor-like sequences) (*34*) and light chain (a histidine-rich region, but proline- rather than glycine-rich). Heparin binding to this molecule is enhanced by Zn^{2+} as well as by decreased pH (*35*). Another example is the effect of zinc on heparin binding by βA4 amyloid precursor protein. The affinity of heparin is increased 2−4-fold by micromolar concentrations of Zn^{2+} (*36*). However, in this case, Zn^{2+} binds to two cysteinyl residues and one glutamate residue (*37*), but not to histidine.

The other motif for heparin binding, which is far more common, consists of basic amino acids (arginine or lysine) displayed on the same side of a helix or β-strand, which requires no metal. These heparin binding domains have been suggested to be defined by linear consensus sequences (*38*). The model of D5 contains no helices, as expected because of the large number of glycines, which are generally thought to be a helix-breaking residue (*39*). It is also possible that the presence of lysine adjacent to histidine may even interfere with zinc binding because of unfavorable electrostatic forces. Six of the seven lysine residues are contiguous in the molecular model based on the NMR structure of hisactophilin (*25*). Conserved motifs are not obvious, and the tertiary structures are probably more important. Moreover, these subdomains differ substantially from each other since the contributions from arginine and lysine to the Zn^{2+}-independent affinities are different.

The first of the proposed motifs of XBBXBX or XBBBXXBX (where B designates a basic residue and X a hydropathic amino acid) is present in H475−K502, namely, in reverse order, XBXBBX, $NK^{491}GK^{493}K^{494}N$. However, a study of fibroblast growth factor 2 (FGF2) using the cocrystal structure of FGF2 and heparin-derived sequences indicates that the tertiary structure may be critical for high-affinity binding (*40*). Indeed, FGF2 consists of 12 antiparallel β-sheets.

HK is known to be one of the important heparin binding proteins in human plasma (*41*). Bjork et al. (*18*) have

localized the ability of HK to slow the heparin-accelerated rate of thrombin inactivation to the light chain (D5 and D6). In this study, we have further delineated the sequence that is responsible for K420−D474 and demonstrated its zinc dependence. This result correlates with the tight binding constant of 3.53 nM for this fragment. In contrast, the C-terminal fragment of D5 and D6, H475−S626, is unable to neutralize the effect of heparin in the antithrombin−thrombin reaction. This difference may be due to the weaker binding constant for heparin (11.9 nM). The concentration of HK in human plasma may be an important modulation of heparin therapy. Under conditions where the level of HK is decreased, e.g., sepsis (*42*), one might expect that a greater sensitivity to heparin might result. However, this situation is complex because of other important heparin-binding proteins such as serum amyloid A, histidine-rich glycoprotein, and platelet-derived PF4 (*41*).

Further knowledge of the relationships of lysine to heparin binding, as well as the contributions of histidine to Zn^{2+} and heparin binding, will depend on the delineation of the three-dimensional structure of D5 in the presence of Zn^{2+}. Efforts to crystallize D5 are in progress.

ACKNOWLEDGMENT

We thank Rita Stewart for expert manuscript preparation. We acknowledge the assistance of Donald Johnson and Elizabeth Eliacin in the cell culture and purification of the recombinant proteins.

REFERENCES

1. Scott, C. F., Silver, L. D., Schapira, M., and Colman, R. W. (1984) *J. Clin. Invest. 73*, 954−962.
2. Auerswald, E. A., Rossler, D., Mentele, R., and Assfalg-Machleidt, I. (1993) *FEBS Lett. 321*, 93−97.
3. Bradford, H. N., Jameson, B. A., Adam, A. A., Wassell, R. P., and Colman, R. W. (1993) *J. Biol. Chem. 268*, 26546−26551.
4. Bradford, H. N., DeLa Cadena, R. A., Kunapuli, S. P., Dong, J. F., Lopez, J. A., and Colman, R. W. (1997) *Blood 90*, 1508−1515.
5. Wachtfogel, Y. T., DeLa Cadena, R. A., Kunapuli, S. P., Rick, L., Miller, M., Schultze, R. L., Altieri, D. C., Edgington, T. S., and Colman, R. W. (1994) *J. Biol. Chem. 269*, 19307−19312.
6. Hasan, A. A. K., Zisman, T., and Schmaier, A. H. (1997) *Thromb. Haemostasis 76*, 141.
7. Puri, R. N., Zhou, F., Hu, C. J., Colman, R. F., and Colman, R. W. (1991) *Blood 77*, 500−507.
8. Kunapuli, S. P., Bradford, H. N., Jameson, B. A., DeLa Cadena, R. A., Rick, L., Wassell, R. P., and Colman, R. W. (1996) *J. Biol. Chem. 271*, 11228−11234.
9. Colman, R. W., White, J. V., Scovell, S., Stadnicki, A., and Sartor, R. B. (1999) *Arterioscler. Thromb. Vasc. Biol. 19*, 2245−2250.
10. Colman, R. W., Pixley, R. A., Najamunnisa, S., Yan, W., Wang, J., Mazar, A., and McCrae, K. R. (1997) *J. Clin. Invest. 100*, 1481−1487.
11. Herwald, H., Dedio, J., Kellner, R., Loos, M., and Mueller-Esterl, W. (1996) *J. Biol. Chem. 271*, 13040−13047.
12. DeLa Cadena, R. A., and Colman, R. W. (1992) *Protein Sci. 1*, 151−160.
13. Gustafson, E. J., Schutsky, D., Knight, L., and Schmaier, A. H. (1986) *J. Clin. Invest. 78*, 310−318.
14. Yung, L. L., Colman, R. W., and Cooper, S. L. (1999) *Blood 94*, 2716−2724.
15. Asakura, S., Hurley, R. W., Skorstengaard, K., Ohkubo, I., and Mosher, D. F. (1992) *J. Cell Biol. 116*, 465−476.
16. Tait, J. F., and Fujikawa, K. (1987) *J. Biol. Chem. 262*, 11651−11656.
17. Lin, Y., Harris, R. B., Yan, W. Y., McCrae, K. R., and Colman, R. W. (1997) *Blood 90*, 690−697.
18. Bjork, I., Olson, S. T., Sheffer, R. G., and Shore, J. D. (1989) *Biochemistry 28*, 1213−1221.
19. Olson, S. T., Francis, A. M., Sheffer, R., and Choay, J. (1993) *Biochemistry 32*, 12148−12159.
20. Olson, S. T., Sheffer, R., and Francis, A. M. (1993) *Biochemistry 32*, 12136.
21. Kunapuli, S. P., DeLa Cadena, R. A., and Colman, R. W. (1993) *J. Biol. Chem. 268*, 2486−2492.
22. Karlsson, R., and Stahlberg, R. (1995) *Anal. Biochem. 228*, 274−280.
23. Habazettl, J., Gondol, D., Wiltscheck, R., Otlewski, J., Schleicher, M., and Holak, T. A. (1992) *Nature 359*, 855−858.
24. Habazettl, J., Schleicher, M., Otlewski, J., and Holak, T. A. (1992) *J. Mol. Biol. 228*, 156−169.
25. Colman, R. W., Jameson, B., Lin, Y., Johnson, D., and Mousa, S. A. (2000) *Blood 95*, 543−550.
26. Dudek, A. Z., Pennell, C. A., Decker, T. D., Young, T. A., Key, N. S., and Slungaard, A. (1997) *J. Biol. Chem. 272*, 31785−31792.
27. Retzios, A. D., Rosenfeld, R., and Schiffman, S. (1987) *J. Biol. Chem. 262*, 3074−3081.
28. Herr, A. B., Ornitz, D. M., Sasisekharan, R., Venkataraman, G., and Waksman, G. (1997) *J. Biol. Chem. 272*, 16382−16389.
29. Kluszynski, B. A., Kim, C., and Faulk, W. P. (1997) *J. Biol. Chem. 272*, 13541−13547.
30. Rojkjaer, R., and Schmaier, A. H. (1999) *Proc. Assoc. Am. Physicians 111*, 220−227.
31. Whitehouse, R. C., Prasad, A. S., Rabbani, P. I., and Cossack, Z. T. (1982) *Clin. Chem. 28*, 475−480.
32. Whitehouse, R. C., Prasad, A. S., and Cossack, Z. T. (1983) *Clin. Chem. 29*, 1974−1977.
33. DeLa Cadena, R. A., Wachtfogel, Y. T., and Colman, R. W. (1994) in *Hemostasis and Thrombosis: Basic Principles and Clinical Practice* (Colman, R. W., Hirsh, J., Marder, V. J., and Salzman, E. W., Eds.) pp 219−240, J. B. Lippincott, Philadelphia.
34. Koide, T., and Odani, S. (1987) *FEBS Lett. 216*, 17−21.
35. Borza, D. B., and Morgan, W. T. (1998) *J. Biol. Chem. 273*, 5493−5499.
36. Multhaup, G., Bush, A. I., Pollwein, P., and Masters, C. L. (1994) *FEBS Lett. 355*, 151−154.
37. Bush, A. I., Multhaup, G., Moir, R. D., Williamson, T. G., Small, D. H., Rumble, B., Pollwein, P., Beyreuther, K., and Masters, C. L. (1993) *J. Biol. Chem. 268*, 16109−16112.
38. Cardin, A. D., and Weintraub, H. J. (1989) *Arteriosclerosis 9*, 21−32.
39. Chou, P. Y., and Fasman, G. D. (1978) *Adv. Enzymol. Relat. Areas Mol. Biol. 47*, 45−148.
40. Wong, P., and Burgess, W. H. (1998) *J. Biol. Chem. 273*, 18617−18622.
41. Williams, E. C., Huppert, B. J., and Asakura, S. (1992) *J. Lab. Clin. Med. 120*, 159−167.
42. Pixley, R. A., Zellis, S., Bankes, P., DeLa Cadena, R. A., Page, J. D., Scott, C. F., Kappelmayer, J., Wyshock, E. G., Kelly, J. J., and Colman, R. W. (1995) *Crit. Care Med. 23*, 41−51.

BI992048Z